Application of Sonie–Schafheitlin Formula and Sampling Theorem in Spectral-Domain Method

Ban-Leong Ooi, Pang-Shyan Kooi, and Mook-Seng Leong

***Abstract*—In this paper, the Sonie–Schafheitlin integration formula and the sampling theorem are integrated into the conventional spectral-domain method to form an efficient and fast convergent hybrid method. As a simple demonstration of the method, the novel technique is applied to the microstrip dispersion problem. The incorporation of the Sonie-Schafheitlin integration formula and the sampling theorem aid to accelerate the convergence of the Sommerfeld integral. Good agreement between the simulated results and the conventional method are obtained.**

***Index Terms*—Sampling theorem, spectral-domain method.**

I. Introduction

The accuracy of the results obtained by the conventional spectral-domain method [1], [2] heavily depends on the accuracy by which the elements of the impedance matrix are evaluated, especially for open structures where these elements are improper integrals with very highly oscillatory tails. Lately, explicit efforts [1]–[4] has been expended in looking for accelerating techniques for fast convergence of the Sommerfeld integral in the spectral-domain method [5]. All these methods require the computation of the Bessel or modified Bessel functions of order greater than one. Hence, they are not efficient in terms of the numerical computation time taken.

In this paper, we propose a modified and fast version of the Uchida method [4] in that, instead of using the higher order spherical Bessel function, only the zeroth-order spherical Bessel function is adopted. By selectively changing the argument of the zero Bessel function such that the zero crossing is identical with the basis function, the integration limit of the residue term of the impedance integral can be made compact and finite. This residue term, which is the substraction of the original impedance integral and the asymptotic term, can be quickly evaluated by any numerical techniques, e.g., [6]. With the Sonie–Schafheitlin integration formula [7] and the sampling theorem, the asymptotic term can be analytically evaluated and the impedance matrix can be made sparse. To validate this new approach, the effective dielectric constant of an open microstrip line is determined and compared to data from the literature. Excellent agreement is documented, along with a considerable reduction in CPU time.

II. Formulation of the Problem

Fig. 1 shows the geometry of the problem, where it is assumed that the thickness of the strip and the metallic ground is negligibly small and the substrate dielectric is lossless.

In contrast with the conventional Galerkin-type spectral-domain method [5], we impose an alternate representation of the boundary condition on the tangential electric field **on the metallic strip** through the following expression:

$$\int_{-\infty}^{\infty}\int_{-\infty}^{\infty}\left\{\vec{E}(x,\ y,\ z=d)p(x)q(y)\right\}e^{-j(\alpha' x+\beta' y)}\,dx\,dy=0 \tag{1}$$

Manuscript received August 10, 1999.

The authors are with the Department of Electrical Engineering, The National University of Singapore, Singapore 119260.

Publisher Item Identifier S 0018-9480(01)00014-X.

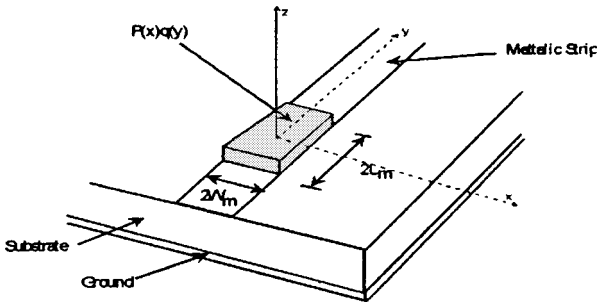

Fig. 1. Geometry of the problem.

where $p(x)$ and $q(y)$ are compact functions that assume zero value outside the metallic strip. The selection of these compact functions are quite arbitrary. For simplicity and convenience, we let

$$p(x)=\begin{cases}1, & |x|\le W_p\\ 0, & \text{elsewhere}\end{cases}\qquad q(y)=\begin{cases}1, & |y|\le L_m\\ 0, & \text{elsewhere}\end{cases}$$

where $2L_m$ is set to one free-space wavelength (see Fig. 1), $W_p = W_m/p$ with $p = 1, 2, 3\ldots$, and W_m is equal to half of the width of the microstrip line. By taking into account the singularities of the surface currents near the edges of the strip, and following the method as in [4] and [5], one would easily arrive at

$$\sum_{\nu=0}^{\infty}\left[A_\nu H_1(k_m,\ \nu,\ W_p)+B_\nu H_2(k_m,\ \nu,\ W_p)\right]=0$$
$$\sum_{\nu=0}^{\infty}\left[A_\nu H_3(k_m,\ \nu,\ W_p)+B_\nu H_4(k_m,\ \nu,\ W_p)\right]=0 \tag{2}$$

where $W_p = W_m/p$ for $n = 2, 3\ldots$,

$$H_1(k_m,\ \nu,\ W_p)=\int_0^{\infty}\frac{\tilde{G}_{xx}(k_m,\ \alpha)J_{\nu+1}(W_m\alpha)j_0(W_p\alpha)\,d\alpha}{W_m\alpha}$$
$$\forall\,\nu=0,\ 2,\ 4,\ \ldots$$
$$=0\qquad\forall\,\nu=1,\ 3,\ 5,\ \ldots$$
$$H_2(k_m,\ \nu,\ W_p)=\int_0^{\infty}\tilde{G}_{xy}(k_m,\ \alpha)J_\nu(W_m\alpha)j_0(W_p\alpha)\,d\alpha$$
$$\forall\,\nu=1,\ 3,\ 5,\ \ldots$$
$$=0\qquad\forall\,\nu=0,\ 2,\ 4,\ \ldots$$
$$H_3(k_m,\ \nu,\ W_p)=\int_0^{\infty}\frac{\tilde{G}_{yx}(k_m,\ \alpha)J_{\nu+1}(W_m\alpha)j_0(W_p\alpha)\,d\alpha}{W_m\alpha}$$
$$\forall\,\nu=1,\ 3,\ 5,\ \ldots$$
$$=0\qquad\forall\,\nu=0,\ 2,\ 4,\ \ldots$$
$$H_4(k_m,\ \nu,\ W_p)=\int_0^{\infty}\tilde{G}_{yy}(k_m,\ \alpha)J_\nu(W_m\alpha)j_0(W_p\alpha)\,d\alpha$$
$$\forall\,\nu=0,\ 2,\ 4,\ \ldots$$
$$=0\qquad\forall\,\nu=1,\ 3,\ 5,\ \ldots. \tag{3}$$

The term $2j_0(k_m L_m)$, which appears in all the series terms in (2), has been eliminated. The unknown propagation constant k_m of the microstrip-line mode is solved in such a way that the determinant of (2) is zero, and the unknown coefficients of the expanded surface currents can also be determined as an eigenvector. In our method, one can tabulate and store the value for $j_0(W_p\alpha)$ in the memory and use it throughout the program. As the resulting impedance is sparse, special techniques like Chio's pivotal condensation method and the Laplace expansion [8] can be used.

III. Numerical Method

To solve the integrals in (3) precisely and without much computation time, the Sonie–Schafheitlin integration formula [7] is utilized for the asymptotic integral. The conventional asymptotic forms of the Green's functions are not used, as this would lead to a singular integrand at the origin for the zeroth-order Bessel function [3]. We propose to use the following expressions for the asymptotic Green's functions:

$$\left[\tilde{G}^{\infty}\right] = \frac{-j\omega\mu}{k_1^2(1+\epsilon_1\epsilon_o)} \begin{bmatrix} \alpha & \beta \\ \beta & \dfrac{-k_1^2(1+\epsilon_1\epsilon_o)+2\beta^2}{2\alpha} \end{bmatrix}. \quad (4)$$

For brevity, only the $Z_{\nu n}^{xx}$ of (3) is given as follows:

$$Z_{\nu n}^{xx} = \int_0^{xa} \frac{\left(\tilde{G}_{xx} - \tilde{G}_{xx}^{\infty}\right) J_{\nu+1}(W_m\alpha) j_0(W_p\alpha)\, d\alpha}{W_m\alpha} + \int_0^{\infty} \frac{\tilde{G}_{xx}^{\infty} J_{\nu+1}(W_m\alpha) j_0(W_p\alpha)\, d\alpha}{W_m\alpha}. \quad (5)$$

The asymptotic terms of (3), $Z_{\nu a}^{ij}$ with $i,\ j = x,\ y$, can, in general, be rapidly solved by the Sonie–Schafheitlin integration formula [7], which is given as follows:

$$\int_0^{\infty} J_{\mu}(t\alpha) J_{\nu}(t\beta) t^{-\lambda}\, dt = \frac{\beta^{\nu}\Gamma\left(\dfrac{\mu+\nu-\lambda+1}{2}\right)}{2^{\lambda}\alpha^{\nu-\lambda+1}\Gamma(\nu+1)\Gamma\left(\dfrac{\mu-\nu+\lambda+1}{2}\right)} \cdot {}_2F_1\left(\frac{\mu+\nu-\lambda+1}{2},\ \frac{\nu-\lambda-\mu+1}{2};\ \nu+1;\ \frac{\beta^2}{\alpha^2}\right) \quad (6)$$

where $0 < \beta < \alpha$, $\mathrm{Re}(\nu+\mu-\lambda+1) > 0$, and $\mathrm{Re}(\lambda) > -1$. In our derivation, it is found that the parameter c in the hypergeometric function ${}_2F_1(a,\ b;\ c;\ z)$ is always equal to 3/2. The hypergeometric function ${}_2F_1(a,\ b;\ (3/2);\ z)$ can be evaluated by (7), shown at the bottom of this page. However, in our proposed approach, we have refrained from using the associated Legendre function, as the evaluation can be very time consuming. We have, instead, adopted the following forms for the asymptotic integrals in (2):

$$\int_0^{\infty} \frac{\tilde{G}_{xx}^{\infty} J_{\nu+1}(W_m\alpha) j_0(W_p\alpha)\, d\alpha}{W_m\alpha} = \frac{-j\omega\mu\sqrt{\pi}\sin\left[(\nu+1)\sin^{-1}\left(\dfrac{W_p}{W_m}\right)\right]}{2\Gamma\left(\dfrac{3}{2}\right) k_1^2(1+\epsilon_1\epsilon_o) W_p W_m(\nu+1)}$$

$$\int_0^{\infty} \tilde{G}_{xy}^{\infty} J_{\nu}(W_m\alpha) j_0(W_p\alpha)\, d\alpha = \frac{-j\omega\mu k_m\sqrt{\pi}\sin\left[\nu\sin^{-1}\left(\dfrac{W_p}{W_m}\right)\right]}{2\nu W_p k_1^2(1+\epsilon_1\epsilon_o)\Gamma\left(\dfrac{3}{2}\right)}$$

$$\int_0^{\infty} \frac{\tilde{G}_{yx}^{\infty} J_{\nu+1}(W_m\alpha) j_0(W_p\alpha)\, d\alpha}{W_m\alpha} = \frac{-j\omega\mu k_m\sqrt{\pi}\Gamma\left(\dfrac{\nu+1}{2}\right)}{4W_m(\nu+2)k_1^2(1+\epsilon_1\epsilon_o)\Gamma\left(\dfrac{3}{2}\right)\Gamma\left(\dfrac{\nu+3}{2}\right)} \cdot \left\{ \cos\left[(\nu+1)\sin^{-1}\left(\frac{W_p}{W_m}\right)\right] + \frac{W_m(\nu+1)\sin\left[\nu\sin^{-1}\left(\dfrac{W_p}{W_m}\right)\right]}{\nu W_p} \right\}$$

$$\int_0^{\infty} \tilde{G}_{yy}^{\infty} J_{\nu}(W_m\alpha) j_0(W_p\alpha)\, d\alpha = \frac{-j\omega\mu\sqrt{\pi}\Gamma\left(\dfrac{\nu}{2}\right)}{16k_1^2(1+\epsilon_1\epsilon_o)(\nu+1)\Gamma\left(\dfrac{\nu+2}{2}\right)\Gamma\left(\dfrac{3}{2}\right)} \cdot \{2k_m^2 - k_1^2(1+\epsilon_1\epsilon_o)\} \cdot \left\{ \cos\left[\nu\sin^{-1}\left(\frac{W_p}{W_m}\right)\right] + \frac{\nu W_m\sin\left[(\nu-1)\sin^{-1}\left(\dfrac{W_p}{W_m}\right)\right]}{W_p(\nu-1)} \right\}. \quad (8)$$

For $\nu = 0$, the fourth integral of (8) is no longer valid and should be replaced by [8]

$$\int_0^{\infty} \tilde{G}_{yy}^{\infty} J_0(W_m\alpha) j_0(W_p\alpha)\, d\alpha = -j\omega\mu W_m K_0(\kappa)\left(2k_m^2 - k_1^2(1+\epsilon_1\epsilon_o)\right)\frac{\sinh\left(\dfrac{W_p\kappa}{W_m}\right)}{2k_1^2\kappa W_p(1+\epsilon_1\epsilon_o)} \quad (9)$$

where κ is an arbitrary real number, $K_{\mu}(z)$ is the modified Bessel functions of the second kind, and

$$\tilde{G}_{yy}^{\infty} = \frac{-j\omega\mu(2k_m^2 - k_1^2(1+\epsilon_1\epsilon_o))\alpha}{2k_1^2(1+\epsilon_1\epsilon_o)\left(\alpha^2 + \left(\dfrac{\kappa}{W_m}\right)^2\right)}.$$

Closed-form equations (8) and (9) are obtained by recursively applying the Gauss's relations for contiguous hypergeometric function. Except for the constant k_m in (8) and (9), these closed-form expressions are evaluated only once at the beginning of the program and stored in the computer's memory. We have intentionally selected $n = 2,\ 3,\ \ldots$, in (2) because (6) is valid for $0 < \beta < \alpha$.

$${}_2F_1\left(a,\ b;\ \frac{3}{2};\ z\right) = \frac{2^{a+b-(5/2)}\Gamma(a-(1/2))\Gamma(b-(1/2))(1-z)^{((3-2a-2b)/4)}\left\{P_{(a-b-(1/2))}^{((3/2)-a-b)}(-\sqrt{z}) + P_{(a-b-(1/2))}^{((3/2)-a-b)}(\sqrt{z})\right\}}{\sqrt{z\pi}} \quad (7)$$

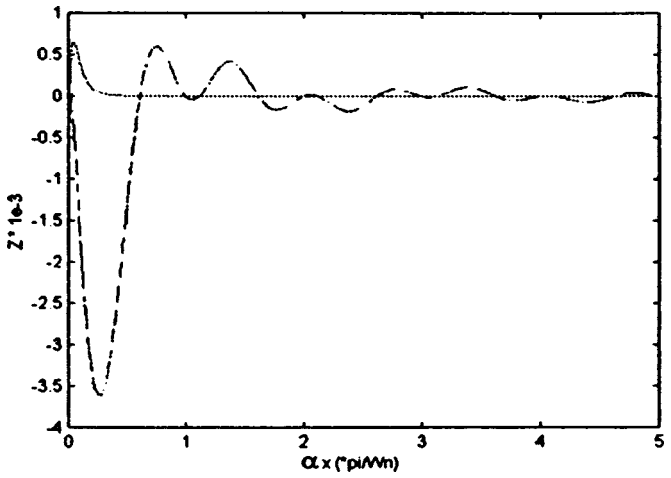

Fig. 2. Typical variation of the complex integrand of $Z_{\nu a}^{xx}$ in (3) for $\nu = 0$, $p = 2$, $\epsilon_1 = 8$, $(W_m/H) = (1/2)$, and $f = 11.8$ GHz (dashed–dotted line: the original integrand without the asymptotic subtraction, solid-line: the integrand $Z_{\nu a}^{xx}$).

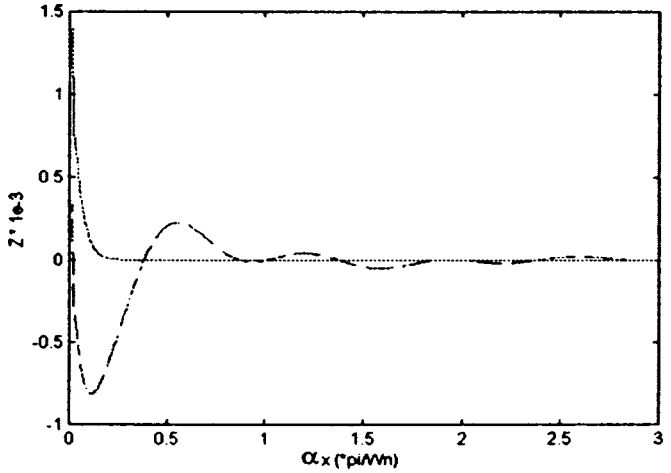

Fig. 3. Typical variation of the complex integrand of $Z_{\nu a}^{xy}$ in (3) for $\nu = 1$, $p = 2$, $\epsilon_1 = 8$, $(W_m/H) = (1/2)$, and $f = 11.8$ GHz (dashed–dotted line: the original integrand without the asymptotic subtraction, solid-line: the integrand $Z_{\nu a}^{xy}$).

IV. Numerical Results

Figs. 2–5 show, respectively, the variations of the integrand $Z_{\nu a}^{xx}$, $Z_{\nu a}^{xy}$, $Z_{\nu a}^{yx}$, and $Z_{\nu a}^{yy}$ with their original integrands that are without the asymptotic substraction. As noticed from these figures, the proposed approach leads to a faster convergence as compared to its original conventional form. A similar trend is also noted for $\nu > 1$, but for brevity, these integrands are not shown. In our experimentation, it is found that an upper limit of $50\pi/W_p$ is sufficient to ensure an accurate evaluation of the integral. Compared with the upper limit in [9], which is given as $\alpha_u = ((1.5\times10^3)/W_m)$, our present method significantly saves much computation time in the numerical integrations.

Fig. 6 compares the convergence rate of the residue term in [3], which is duplicated as follows:

$$\int_0^\infty \frac{\left(\tilde{G}_{xx} - \tilde{G}_{xx}^{\infty}\right) J_{\nu+1}^2(W_m\alpha)}{W_m\alpha}\, d\alpha \tag{10}$$

with our proposed $Z_{\nu a}^{xx}$. Here, ν is taken as ten and this comparison is done on the basis that $Z_{\nu a}^{xx}$ and (10) occupy the same matrix element

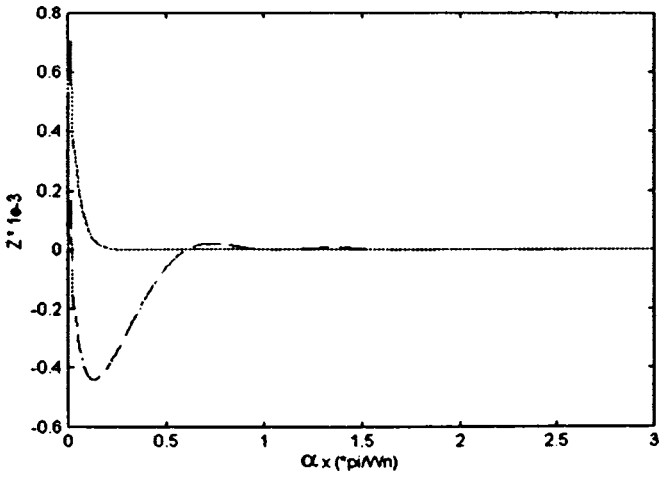

Fig. 4. Typical variation of the complex integrand $Z_{\nu a}^{yx}$ in (3) for $\nu = 1$, $p = 2$, $\epsilon_1 = 8$, $(W_m/H) = (1/2)$, and $f = 11.8$ GHz (dashed–dotted line: the original integrand without the asymptotic subtraction, solid-line: the integrand $Z_{\nu a}^{yx}$).

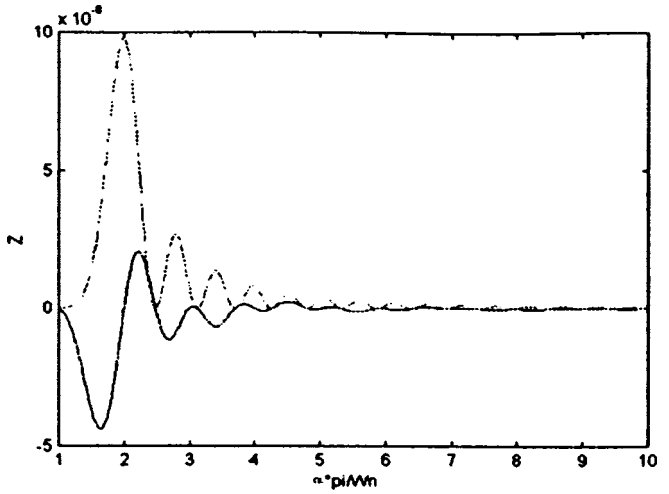

Fig. 5. Typical variation of the complex integrand $Z_{\nu a}^{yy}$ in (3) for $\nu = 0$, $p = 2$, $\epsilon_1 = 8$, $(W_m/H) = (1/2)$, and $f = 11.8$ GHz (dashed–dotted line: the original integrand without the asymptotic subtraction, solid-line: the integrand $Z_{\nu a}^{yy}$).

position. As shown from the figure, our approach has a faster decaying envelope than that in [3]. The selection of the zeroth-order spherical Bessel function with p as the only degree of freedom has caused the tail of the original integrand to diminish faster than using the Bessel function. A similar trend has also been observed for all the other impedance matrix elements, but for brevity, they are not shown in this paper. By making p the varying element in this non-Galerkin method, the need to evaluate the spherical Bessel function of an order higher than zero, as in [4], is removed. As such, the computation time will improve significantly.

A program written in MATLAB 5 is used to implement the algorithm for the microstrip dispersion problem. The quasi-static effective permittivity is computed as an initial guess and the Newton method is used to find the root of the characteristic equation representing the dominant mode. The effective dielectric constant of a microstrip line of aspect ratio $2W_m/H = 1$ was determined for different values of the ratio H/λ_0. Table I summarizes the results obtained from this paper and those presented in [3] and [10]. Here, five basis functions are taken

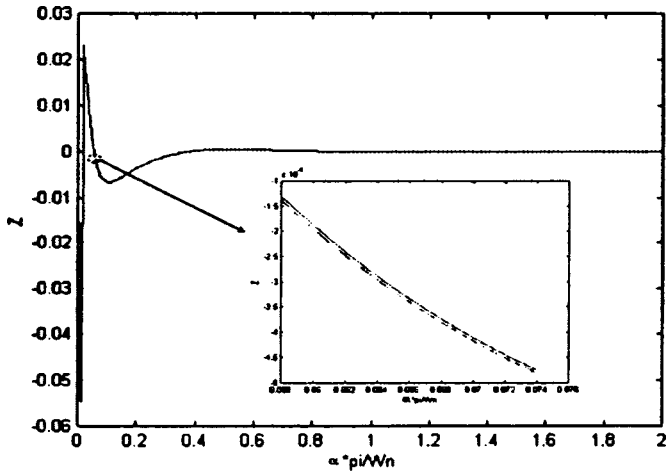

Fig. 6. Comparison of $Z_{\nu\alpha}^{xx}$ and (10). $\nu = 10$, $p = 10$, $\epsilon_1 = 8$, $(W_m/H) = (1/2)$, and $f = 11.8$ GHz (dashed–dotted line: for (10), solid-line: our proposed method $Z_{\nu\alpha}^{xx}$).

TABLE I
EFFECTIVE DIELECTRIC-CONSTANT COMPARISON WITH $\epsilon_1 = 8$, $2W_m/H = 1$, and $\mu_r = 1$

$\frac{H}{\lambda_o}$	This work	[3]	[10]
0.005	5.4678	5.4678	5.4752
0.05	6.1274	6.1275	6.1316
0.1	6.7582	6.7580	6.7572
0.3	7.661	7.6614	7.6551
0.7	7.9133	7.9139	7.9151
1.0	7.9529	7.9529	7.9556

for both J_x and J_y. The agreement between this paper and that presented in [3] is excellent. The total time taken to compute the effective dielectric constant for the case of $H/\lambda_o = 1$ is 4 s on a Pentium 400-MHz personal computer.

V. CONCLUSION

In this paper, the Sonie–Schafheitlin integration formula and the sampling theorem have been integrated into the conventional spectral-domain method to form an efficient and fast convergent hybrid method. Closed-form asymptotic integrals are first derived without introducing any numerical pathologies and complexities. Numerical results obtained from this approach agree very well with those reported in the literature. A substantial reduction in CPU time is also achieved using this formulation.

REFERENCES

[1] S. O. Park and C. A. Balanis, "Analytical technique to evaluate the asymptotic part of the impedance matrix of Sommerfeld-type integrals," *IEEE Trans. Antennas Propagat.*, vol. 45, pp. 798–805, May 1997.
[2] ——, "Dispersion characteristic of open microstrip lines using closed-form asymptotic extraction," *IEEE Trans. Microwave Theory Tech.*, vol. 45, pp. 458–460, Mar. 1997.
[3] S. Amari, R. Vahldieck, and J. Bornemann, "Using selective asymptotics to accelerate dispersion analysis of microstrip lines," *IEEE Trans. Microwave Theory Tech.*, vol. 46, pp. 1024–1027, July 1998.
[4] K. Uchida, T. Noda, and T. Matsunaga, "New type of spectral-domain analysis of a microstrip line," *IEEE Trans. Microwave Theory Tech.*, vol. 37, pp. 947–952, June 1989.
[5] T. Itoh, "Spectral domain immittance approach for dispersion characteristics of a generalized printed transmission lines," *IEEE Trans. Microwave Theory Tech.*, vol. MTT-28, pp. 733–736, July 1980.
[6] B. L. Ooi, P. S. Kooi, and M. S. Leong, "Efficient evaluation of singular and infinite integrals using the ERF transform," *IEEE Trans. Antennas Propagat.*, submitted for publication.
[7] G. N. Watson, *A Treatise on the Theory of Bessel Functions*. Cambridge, U.K.: Cambridge Univ. Press, 1962.
[8] I. S. Gradshteyn and I. M. Ryzhik, *Table of Integrals, Series, and Products*. New York: McGraw-Hill, 1962.
[9] M. Kobayashi and F. Ando, "Dispersion characteristics of open microstrip lines," *IEEE Trans. Microwave Theory Tech.*, vol. MTT-35, pp. 101–105, Feb 1987.
[10] S. O. Park and C. A. Balanis, "Dispersion characteristics of open microstrip lines using closed-form asymptotic extraction," *IEEE Trans. Microwaves Theory Tech.*, vol. 45, pp. 458–460, Mar 1997.

Scattering Matrices Representing the Transformations Between Modal Bases in Rectangular Waveguide

A. Morini, T. Rozzi, and L. Zappelli

***Abstract*—The excitation of hybrid modes by discontinuities in rectangular waveguide can often be decomposed into separate LSE/LSM or TE/TM mechanisms, so that each component can be analyzed with the most suitable modal base. Correct interfacing, however, is required. We report the scattering matrices representing all the possible transformations of modal bases in rectangular waveguide. Such matrices provide an useful tool to simulate complex circuits made up of components strongly interacting, without requiring the use of a common modal base for the characterization of each element. Since the transformation matrices can easily include pieces of transmission lines, their use does not require any additional computation effort.**

***Index Terms*—Mode matching, rectangular waveguides.**

I. INTRODUCTION

The electromagnetic (EM) field into a rectangular waveguide can be expanded into three different sets of modes, namely $\mathbf{H}$ and $\mathbf{E}$ types with respect to $\hat{\mathbf{x}}$, $\hat{\mathbf{y}}$, and $\hat{\mathbf{z}}$ (the latter are the classical TE/TM modes). However, although in principle any one is equivalent to another, in practical use, the analysis and computation effort required to characterize monodimensional discontinuities, such as T/Y-junctions, inductive or capacitive posts and windows, bends, tapers, and so on (see Fig. 1) is strongly reduced when the most appropriate set is used [1]. The latter is the one whose modes are derived from two potentials ($\mathbf{H}$ and $\mathbf{E}$) parallel to the axis of the discontinuity (that is, the one with respect to which the discontinuity is uniform). As a consequence, the complete analysis of the discontinuity can be performed considering separately the two families of modes ($\mathbf{E}$ and $\mathbf{H}$), as not being coupled at all by the discontinuity.

Consequently, the EM problem posed by such structures reduces to a scalar one, as the continuity condition at the discontinuity interface involves only one potential directed along one coordinate and its first derivative at a time.

On the other hand, in complex structures, there are many discontinuities and components connected together and often strongly interacting through higher order modes. A classical example of this situation is of-

Manuscript received January 13, 2000. This work was supported in part by the Agenzia Spaziale Italiana.

The authors are with the Dipartimento di Elettronica ed Automatica, Universita di Ancona, I-60131 Ancona, Italy.

Publisher Item Identifier S 0018-9480(01)00004-7.